Control of Linear Dampers for Large Space Structures

J. K. Haviland,* T. W. Lim,† W. D. Pilkey‡, and H. Politansky§
University of Virginia, Charlottesville, Virginia 22901

This paper addresses the problem of designing a control system for a linear proof-mass damper (actuator) for large space structures. Initially, a linear control law is developed for a self-contained damper. The linear control law shows that although adequate damping can be achieved at high frequencies, very little damping can be obtained at frequencies of 1 Hz or less, because stops must be set to limit the motion of the proof mass. To improve the actuator performance at low frequencies, this paper considers the limiting performance method and its application to control problems. In a preliminary study, the optimal response is calculated for a single-degree-of-freedom model of a cantilever beam controlled by a proof-mass damper using a limiting-performance/minimum-time formulation. It is shown that considerable damping can be achieved at low frequencies. Also, parameter identification is used to find a suboptimal feedback control law based on the limiting performance characteristics. There is an important difference in the way that the last two methods handle elastic impacts between the proof mass and the stops. The limiting-performance-method solution brings the relative motion to rest before impact occurs by applying the appropriate forces. However, in the suboptimal case, the proof mass can strike the stops since the dynamics of elastic impact are modeled.

Introduction

MANY studies of the problems of controlling large space structures have been performed. Because of requirements for low-weight, accurate positioning, and rapid variation suppression, much research has been focused on designing active vibration control systems for such structures.[1] To achieve active control systems, several designs for damping actuators have been proposed that would augment the natural damping of structures. Such designs have included gyrodampers, inertia wheels, linear dampers, and pivoted proof-mass actuators. A pivoted proof-mass actuator, which is similar dynamically to a linear damper, was employed for the structural control of a circular plate by Aubrun, Ratner, and Lyons.[2] One version of a linear proof-mass actuator is the linear d.c. motor (LDCM) that has recently been studied extensively in relation to the NASA Control of Flexible Structures (COFS) program.[3-7] Another version is based on a magnetic yoke driven by a fixed coil. A prototype of such a system was designed at the University of Virginia for NASA, and its dynamical behavior was evaluated by Zimmerman et al.[8]

In the present work, a linear control law is first developed for a prototype proof-mass damper. The damper is designed to be self-contained and to provide damping over the full frequency range regardless of the nature of the controlled structure, while insuring a centering force for the proof mass. Although adequate damping can be achieved at the higher frequencies, it proved ineffective below frequencies of a few hertz when practical design constraints are used. These results appear to be consistent with the observations made by Ham et al. who studied the control of a LDCM based on a positive-real decentralized velocity feedback (PRDVF) controller. There are several possible ways by which the low-frequency performance of the proof-mass damper might be improved, including improving the filtering of the accelerometer signal, using the optimal nonlinear feedback method,[9] or using electronic limiters. Yet another approach might be the application of the limiting-performance method.

The limiting-performance method in its application to proof-mass dampers was discussed earlier[10,11] and is considered further here. With this method, the optimal control force and response variable trajectories can be calculated as a function of time for a known system and given initial conditions, subject to certain constraints and external excitations, while minimizing a given performance index. This method has been used in design tradeoff studies for shock isolation systems.[12] Since a major concern with the control of large space structures is the rapid suppression of the vibrations, minimum-time solutions are superimposed on the limiting-performance control in the present work, i.e., the optimal response is selected that reduces the peak response to within a prescribed limit in the minimum time. Numerical results are quite promising, but the computational load is heavy, and difficulties in building a control system in real time can be expected. The control scheme using the limiting-performance method is open-loop control, i.e., the optimal control and the state variables are computed in terms of time. Although the results of a limiting performance analysis give useful information to a designer on the optimal performance of the system, it may prove difficult to implement such a control system when the parameters of the model are uncertain and the system is subject to unknown disturbances. Therefore, a closed-loop control[13] has been developed that is relatively robust to the unknowns in the system. To establish a suboptimal feedback control law based on the limiting performance characteristics, a parameter identification technique using gains from the algebraic Riccati equation is considered here.

Design of a Proof-Mass Damper

One of several designs for a linear proof-mass damper is shown in Fig. 1. It incorporates two doughnut-shaped samarium-cobalt magnets and an annular soft-iron yoke that combines the functions of moving mass and magnet. This assembly moves over a fixed coil carrying a current controlled to produce the required force on the magnet and, thus, the

Presented as Paper 87-2251 at the AIAA Guidance, Navigation, and Control Conference, Monterey, CA, Aug. 17-19, 1987; received Jan. 19, 1988; revision received Oct. 10, 1988.

*Professor, Department of Mechanical and Aerospace Engineering. Associate Fellow AIAA.
†Graduate Research Assistant, Department of Mechanical and Aerospace Engineering.
‡Professor, Department of Mechanical and Aerospace Engineering.
§Visiting Scholar, Department of Mechanical and Aerospace Engineering; also, Rafael, Ministry of Defense, Israel.

required reaction on the structure to be damped. The magnetic yoke moves on linear bearings along a stainless steel rod so that the design is limited not only by the size of magnets available, but also by the sizes of the linear bearings available. The coil size is also limited by the size of annular gap that can be provided in the yoke. Given this coil size, the maximum force available is limited by the current that can be carried by the coil without overheating. It was assumed that friction in the linear bearings would be sufficiently small that it could be ignored. However, experience in the laboratory shows that friction can become a significant parameter at low frequencies under the linear control laws.

In the prototype design, a maximum force of 192 N was achieved over a travel of ± 0.0127 m (a total range of 1 in.). The force was limited by the total effective flux of 91 μWe, which can possibly be increased by about 20% with a better yoke design. The travel was a compromise based on the resistance of the coil winding and the driving voltage available, a greater travel could be obtained at the expense of greater power dissipation in the longer coil. In the design chosen, the coil had a resistance of 8 Ω and was limited to a steady current of 1 A. The mass of the moving yoke is 0.278 kg.

The design provided for two sensors: an accelerometer attached to the damper in a fully collocated application, and a sensor to measure the relative position of the proof mass within the housing. The accelerometer must be of the servo type because it must provide control signals down to zero frequency, whereas the position sensor is essential if the effects of striking against the stops that limit travel were to be avoided. In the design shown in Fig. 1, a linear variable differential transformer (LVDT) is used. However, an alternative sensor that has also been used quite successfully incorporates a tapered aluminum sleeve shrunk over the yoke (as an alternative, the yoke could be tapered during manufacture) used in conjunction with a proximeter (which measures the distance to a conducting surface).

Linear Control Laws

The linear control laws are designed under the assumption that the damper will be attached at any location on a structure

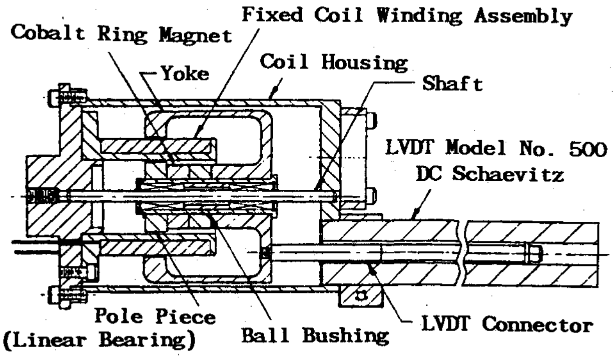

Fig. 1 Linear proof-mass damper.

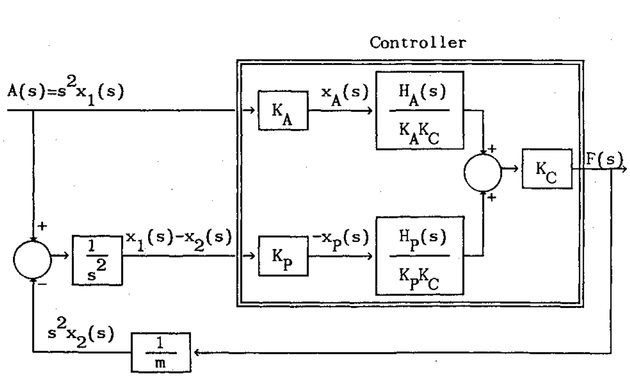

Fig. 2 Block diagram of linear controller.

and that it will provide a positive real coefficient of damping to that structure. The following discussion focuses on analog control laws, with the assumption that the results will be almost identical to those for a digital system at frequencies of around 1 Hz.

A block diagram of the damper is shown in Fig. 2. The input is the acceleration $A(s)$ of the structure (from the accelerometer), and the output is the force $F(s)$ acting on the proof mass with an equal and opposite reaction acting on the structure. Thus the complex damping $H_C(s)$ is

$$H_C(s) = \frac{F(s)}{A(s)/s} \tag{1}$$

It can be shown that as long as the real part of the complex damping is positive over the entire frequency spectrum, the damper can only absorb energy.

The two blocks marked K_A and K_P in Fig. 2 represent the accelerometer and proximeter (or LVDT), respectively, as well as associated calibration amplifiers and analog-to-digital converters when a digital controller is used. These are calibrated so that the full range of the controller is obtained with ± 9.8 m/s^2 input from the accelerometer (calibrated by holding the accelerometer vertical, and then inverting it), and ± 0.0127 m from the proximeter (calibrated by moving the proof mass from one stop to the other), It is, of course, important to be able to set these ranges easily so that the correct gains can be obtained. The block marked K_C represents the combined output amplifier and the electromagnetic properties of the coil and yoke; this was actually a pulse-width modulator driven by digital signals in one control application, whereas a current amplifier driven through a digital-to-analog converter was used in another control application. The output gain is set so that the full controller range results in the maximum range of force output, which is ± 1.92 N. The two transfer functions in the blocks marked $H_A(s)/K_AK_C$ and $H_P(s)/K_PK_C$, together with the summation block, are included in the digital program of the controller. A more complex block diagram was also investigated that included the effects of coil inductance and of back emf, but these were found to have very little effect on the damping at low frequencies. The two transfer functions shown in Fig. 2 were chosen as follows.

The accelerometer signal is integrated by H_A to provide a damping force proportional to velocity, while providing sufficient force on the proof mass to prevent motion relative to the stops in a steady acceleration. A simple function that can do this is

$$H_A(s) = \frac{m}{1 + s/\omega_A} \tag{2}$$

A pseudospring stiffness with a given phase margin is provided by H_P.

$$H_P(s) = k\,\frac{1 + s/\omega_V}{1 + s/\omega_Y} \tag{3}$$

In the preceding equations, m is the proof mass (0.278 kg), and $\omega_A = c/m$ is a break frequency that determines the value for c, the asymptotic value for the damping at high frequencies, otherwise referred to as the design damping. Also, k is the equivalent centering spring stiffness, while the pole and zero in $H_P(s)$ can be located to provide a given phase margin. The nominal value for k is set at 38 N/m, whereas the values used for the other parameters are based on laboratory experience. Using the definition of Eq. (1) and analyzing the block diagram in Fig. 2,

$$H_C(s) = \frac{s[H_A(s) + H_P(s)/s^2]}{1 + H_P(s)/ms^2} \tag{4}$$

When the definitions of Eqs. (2) and (3) are used, the real part of the preceding function Real$\{H_C\}$ is positive over the entire frequency range, which insures stability regardless of

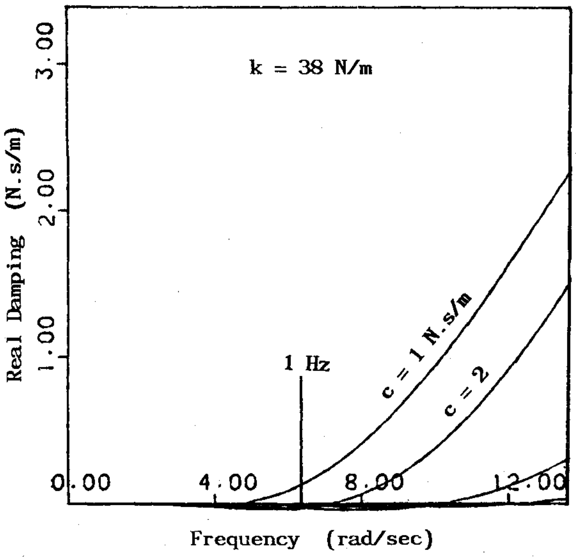

Fig. 3 Real damping for linear laws with nominal k.

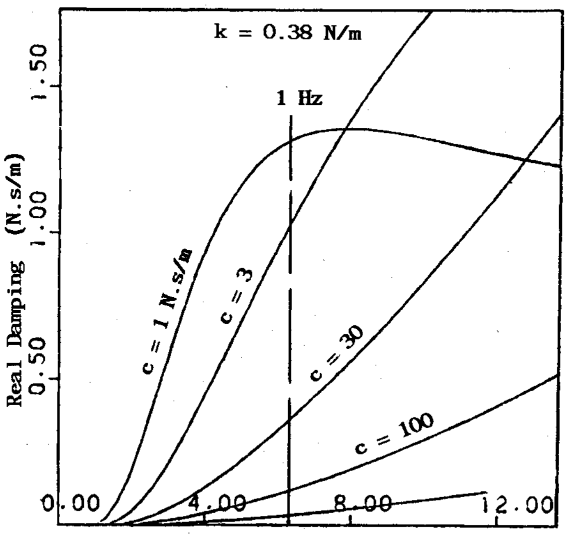

Fig. 4 Real damping for linear laws with reduced k.

the natural frequencies of any passive structure to be damped. Another function of interest is the ratio of the relative motion (x_1-x_2) to the structural motion x_1. This can be expressed as

$$R_C(s)=\frac{s^2(x_1-x_2)}{A(s)}=\frac{1-H_A(s)/m}{1+H_P(s)/ms^2} \tag{5}$$

The magnitude of this function $|R_C|$ indicates the ratio of the amplitude of the motion of the yoke in the housing to the amplitude of the structural displacement at the given frequency. Therefore, for one unit of total travel, its reciprocal gives the permissible structural amplitude, assuming that the control law is to remain linear.

Linear s-Plane Analysis

The two functions Real$\{H_C\}$ and $|R_C|$ can be evaluated for various values of the parameters c (damping) and k (synthetic stiffness). Plots of Real$\{H_C\}$ against frequency are given in Fig. 3 for various values of design damping c and for the nominal value of k; this shows very low values at frequencies around 1 Hz. Also, the lower values for Real$\{H_C\}$ appear to occur with the highest values of the design damping parameter c. The corresponding plots for $|R_C|$ (not shown) indicate

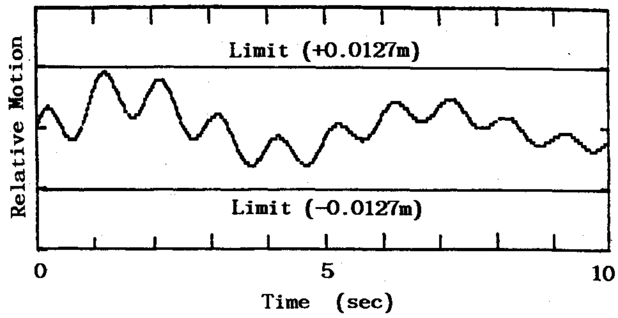

Fig. 5 Linear law simulation of relative motion with reduced stiffness.

that the relative amplitudes of the yoke are very small under these conditions, so that the problem cannot be attributed to the restrictions on the travel of the proof mass. Plots of Real$\{H_C\}$ are also shown in Fig. 4 for a synthetic stiffness k of one-hundredth of the nominal value (0.38 N/m); this shows considerably improved damping; however, the probability that the yoke will strike the stops is greatly increased.

Analysis of Equations of Motion

In order to study the response of the proof mass at low frequencies with the linear control law, the equations of motion are integrated numerically, with the self-contained proof-mass damper attached to a mass-spring system having a natural frequency of 1 Hz, but without the effects of friction. A plot of the results is shown in Fig. 5 with the reduced value of k (0.38 N/m) and with an initial impact to the yoke. In this plot, two periods appear superimposed, the 1-s period of the structure and the 5.3-s period of the yoke mass under a weak synthetic spring. Although the simple mass-spring structure is damped, the yoke comes close to striking the stops.

The limiting performance is defined as the minimum peak value of a certain response while other system responses are constrained. Since the minimum-maximum norm of the limiting-performance method gives unique response trajectories only until the peak value of the performance index is reached, additional performance measures are employed in order to provide the unique trajectories after the peak. These unique trajectories are chosen to reduce the peak value within a prescribed limit in minimum time. The resulting characteristics are referred to as the limiting-performance/minimum-time (LP/MT) characteristics. These LP/MT characteristics are applied to the control of proof-mass dampers.

Problem Statement for the LP/MT Characteristics

A linear vibrating system with n degrees of freedom subject to arbitrary external excitations $f(t)$ and control forces $u(t)$ is represented by the first-order system of differential equations

$$\dot{s}(t)=As(t)+Bu(t)+Cf(t) \tag{6}$$

where $s(t)$ is a $2n$-dimensional state vector, while A, B, and C are $2n\times 2n$, $2n\times n_u$, and $2n\times n_f$ constant coefficient matrices, respectively. The quantities n_u and n_f are the number of control forces and excitations, respectively. In general, the measures of performance and of the constraints may be linear combinations of state variables, control forces, and external excitation. Since the trajectory after the peak is required to be reduced within a prescribed limit in minimum time, the performance index J to be minimized is

$$J=J_t+J_s \tag{7}$$

where J_t and J_s are referred to as the transient performance index and the steady-state performance index, respectively.

Define these two performance indices as

$$J_t = \max_{t_0 \le t < t_t} [p_1^T s(t) + p_2^T u(t) + p_3^T f(t)] \quad (8)$$

$$J_s = \max_{t_t \le t \le t_f} [p_1^T s(t) + p_2^T u(t) + p_3^T f(t)] \quad (9)$$

where t_0 and t_f are given initial and final times; t_t is the assumed minimum time that is to be found iteratively, and p_1, p_2, and p_3 are prescribed $2n$, n_u, and n_f constant coefficient vectors, respectively. Note that the same p_1, p_2, p_3 are used in both performance indices. The transient performance index is used to give a unique response trajectory up to the point of the peak value, and the steady-state performance index is used to reduce the response trajectory after the peak within a prescribed value in minimum time. The prescribed value may be arbitrarily selected by a designer to meet the design specification.

Constraints are imposed on the dynamic system under study. To reduce the response in minimum time, consider two sets of constraints. One set of constraints, referred to as the transient constraints, is used to represent the constraints from t_0 to t_t

$$y_{tl} \le Q_1 s(t) + Q_2 u(t) + Q_3 f(t) \le y_{tu} \quad \text{for} \quad t_0 \le t \le t_t \quad (10)$$

Here y_{tl} and y_{tu} are n_c-dimensional lower and upper constraint vectors, and Q_1, Q_2, and Q_3 are $n_c \times 2n$, $n_c \times n_u$, and $n_c \times n_f$ constant coefficient matrices. The quantity n_c is the number of constraints. An additional constraint set, referred to as steady-state constraints, is imposed from t_t to t_f

$$y_{sl} \le Q_1 s(t) + Q_2 u(t) + Q_3 f(t) \le y_{su} \quad \text{for} \quad t_t \le t \le t_f \quad (11)$$

where y_{sl} and y_{su} are n_c-dimensional coefficient vectors representing lower and upper bounds of steady-state constraints. The steady-state constraints represent the prescribed values of the responses after the peak. Note that the matrices Q_1, Q_2, and Q_3 in Eq. (11) are identical to those in Eq. (10).

With these definitions, the optimization problem is to find optimal control forces $u^*(t)$ with the smallest t_t that will meet the following criteria: 1) the peak value of the response selected in the transient performance index is unique, 2) the peak value of the response selected in the steady-state performance index stays within the prescribed value, and 3) the transient and the steady-state constraints are satisfied.

Linear Programming Formulation

Consider now the linear programming formulation of the previously stated problem. If the system in Eq. (6) is discretized using N uniform time intervals, a set of state difference equations is obtained for $k = 1,2,\ldots, N$

$$s(t_k) = Gs(t_{k-1}) + H[Bu(t_k) + Cf(t_k)] \quad (12)$$

where

$s(t_k)$	= state vector at time $t_k = kh$
$u(t_k)$, $f(t_k)$	= control and external excitation vectors, assumed to be constant over the interval $t_{k-1} < t \le t_k$
G	$= e^{Ah}$
H	$= \int_0^h e^{A(h-\tau)}\, d\tau$
h	= time interval $= t_k - t_{k-1}$

The state vector $s(t_k)$ can be expressed at any time $t = t_k$ as a function of the initial state $s(t_0)$, the control history $u(t_1)$, $u(t_2),\ldots, u(t_N)$ and the external excitation $f(t_1), f(t_2),\ldots, f(t_N)$. For $k = 1,2,\ldots, N$

$$s(t_k) = G^k s(t_0) + \sum_{j=1}^{k} G^{k-j} H[Bu(t_j) + Cf(t_j)] \quad (13)$$

The peak values of Eqs. (8) and (9), which reflect the minimum-maximum norms, can be converted into constraints. Since J_t is the peak value of $[p_1^T s + p_2^T u + p_3^T f]$ for $t_0 \le t < t_t$, and J_s serves the same purpose for $t_t \le t \le t_f$, the constraints from the performance index when discretized using N uniform intervals are

$$[p_1^T s(t_k) + p_2^T u(t_k) + p_3^T f(t_k)] \le J_t \quad \text{for} \quad k = 1,2,\ldots, N_t - 1 \quad (14)$$

and

$$[p_1^T s(t_k) + p_2^T u(t_k) + p_3^T f(t_k)] \le J_s \quad \text{for} \quad k = N_t, N_t + 1,\ldots, N \quad (15)$$

where N_t is the discretized time t_t. The two sets of constraints (10) and (11) can also be discretized using N uniform intervals. Upon substitution of Eq. (13) into the discretized constraint equations, the control sequence $u(t_k)$ becomes the only set of unknowns.

To place this optimization problem into a standard linear programming form, define

$$z = \begin{bmatrix} J_t \\ J_s \\ \underline{u} \end{bmatrix} \quad (16)$$

where

$$\underline{u} = [u(t_1), u(t_2),\ldots, u(t_N)]^T \quad (17)$$

$$c^T = [1\ 1\ 0\ \ldots\ 0] \quad (18)$$

Then the linear programming problem is to minimize

$$J = c^T z \quad (19)$$

subject to the constraints

$$Hz \le b \quad (20)$$

where H and b are a coefficient matrix and a coefficient vector, respectively, representing constraints of Eq. (10), (11), (14), and (15). This linear programming problem is solved iteratively with the prescribed constraints, the given steady-state performance index, and a trial value of N_t until the smallest value of N_t is obtained satisfying the criteria given in the problem statement. To find the smallest N_t efficiently, an interpolation method such as the bisection method or the secant method[15] may be employed.

Application of Linear Programming to a Proof-Mass Damper

Consider the clamped-free uniform beam shown in Fig. 6. A proof-mass damper is attached at the free end of the beam. A single-degree-of-freedom model of the cantilever beam representing only the first natural frequency is used. The mass of the housing of the proof-mass damper is neglected. The equivalent single degree-of-freedom model with a proof-mass damper is shown in Fig. 7. The resulting equation of motion is

$$M\ddot{x}_1 + Kx_1 - u = 0$$

$$m\ddot{x}_2 + u = 0 \quad (21)$$

where M and K are the equivalent mass and stiffness of the beam, respectively; m is the mass of the proof mass, and u represent the control force of the proof-mass damper. Because of physical limitations, the proof-mass damper has constraints on the distance that it can travel and the force that can be generated.

$$|d| = |x_2 - x_1| < d_{\max}, \qquad |u| \le u_{\max} \quad (22)$$

Impact dynamics are not included in these equations because the forces calculated by linear programming during the solution are sufficient to bring the relative motion to zero just before impact would have occurred. Plots of the solutions show the proof mass just short of the stops for a finite period., The proof mass finally moves away at the optimum time.

Based on the configuration of the prototype proof-mass damper, the parameters are determined to be $d_{max} = 1.27 \times 10^{-2} m$, $u_{max} = 2N$, $m = 0.278$ kg, $M = 2.78$ kg. Also the natural frequency of the beam, to represent a typical low-frequency value, is selected as $\omega = \sqrt{K/M} = 2\pi$ rad/s = 1 Hz. Assume that the system is at rest initially and the mass M is subject to initial displacement $x_1(0) = 0.01$ m. Introduce the state vector $s = [x_1 \, \dot{x}_1 \, d \, \dot{d}]^T$. Then a set of first = order differential equations is obtained.

$$\dot{s} = As + Bu \tag{23}$$

where

$$A = \begin{bmatrix} 0 & 1 & 0 & 0 \\ -\omega^2 & 0 & 0 & 0 \\ 0 & 0 & 0 & 1 \\ \omega^2 & 0 & 0 & 0 \end{bmatrix}, \qquad B = \begin{bmatrix} 0 \\ 1/M \\ 0 \\ -\dfrac{M+m}{Mm} \end{bmatrix} \tag{24}$$

with initial conditions

$$s(0) = [0.01 \quad 0 \quad 0 \quad 0]^T \tag{25}$$

The peak displacement of the mass M is to be minimized, and the subsequent response is to be reduced to a prescribed level, 2% of the initial displacement, in minimum time. Thus, the performance index is to minimize

$$J = J_t + J_s \tag{26}$$

where

$$J_t = \max_{0 \le t < t_t} |x_1(t)| \tag{27}$$

$$J_s = \max_{t_t \le t \le t_f} |x_1(t)| \tag{28}$$

The steady-state performance index is prescribed as $J_s = 0.2 \times 10^{-3}$m. The constraints of Eq. (22) are applied for $0 \le t \le t_f$. Now, the problem is to find the optimal $u^*(t)$ and the smallest t_t that will meet the following criteria: 1) the performance index J is minimized, 2) the steady-state performance index stays within the prescribed value, and 3) the constraints are satisfied. Since the response is sinusoidal and the natural frequency of the mass-spring system is 1 Hz, the period $T = 2\pi/\omega = 1$ s. Thus, $(N - N_t)h$ is chosen to be 0.5 s. Discretization in time h is taken to be 0.05 s. The resulting minimum time is $t_t = 2.05$ s, and the performance index is $J = J_t + J_s = 0.01 + 0.0001 = 0.0101$ m. Figure 8 shows the resulting time responses. From the limiting performance response it is noted that a highly satisfactory damped response is achieved as the best "limiting" solution to the proof-mass control problem at 1 Hz with the given conditions.

System Identification

Since the limiting-performance method gives the best possible response of a system, it may be reasoned that a control system based on the limiting-performance characteristics will be the best. However, due to uncertainties in control problems, open-loop control such as the limiting-performance control may not be applicable in practice. On the other hand, the optimal control theory provides stable feedback control laws that are valuable in practical applications. It is difficult to use the optimal control theory to derive feedback control laws when a system is subject to constraints; however, limiting performance methods can be used readily for control problems subject to constraints. Therefore, parameter identification can be used to find suboptimal feedback control laws based on the limiting-performance characteristics, thereby making use of the benefits of the two control methods.

Limiting-Performance Characteristics

The first step in identifying suboptimal feedback control parameters is to compute the LP/MT characteristics. Consider the proof-mass damper control problem treated previously. Assume that the expected external excitation will not excite the elastic mode of the system above the energy level that is achievable by the initial conditions in Eq. (25).

Parameter Identification

Taking the LP/MT solution as optimal, a suboptimal solution $s^*(t)$ is found by numerical solution of Eq. (6), i.e., by solution of

$$\dot{s}^*(t) = As^*(t) + Bu^*(t) \tag{29}$$

subject to the constraints of Eq. (22) together with elastic boundary conditions on impact. Elastic impacts are represented by reversing the fourth term $\dot{d}$ in the state vector $\dot{s}^*(t)$ whenever $d = \pm d_{max}$, and then adjusting the second term $\dot{x}_1$ to conserve momentum. Limitations on the control force are represented by

$$u_s^*(t) = \begin{cases} u_{max} & \text{for} \quad u_s(t) > u_{max} \\ u_s(t) & \text{for} \quad |u_s(t)| \le u_{max} \\ -u_{max} & \text{for} \quad u_s(t) < -u_{max} \end{cases} \tag{30}$$

where

$$u_s(t) = -G_s^*(t) \tag{31}$$

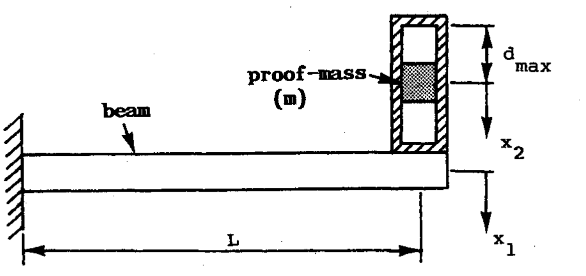

Fig. 6 A cantilever beam controlled by a proof-mass damper.

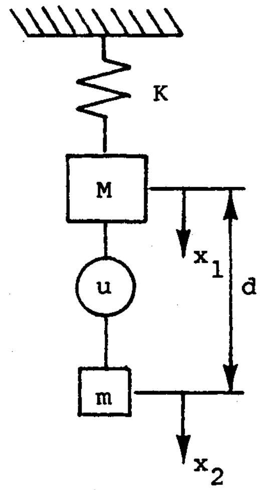

Fig. 7 Single-degree-of-freedom model of the cantilever beam with the proof-mass damper.

and G is the constant feedback gain matrix that is to be found.

Define the difference between the suboptimal force and the optimal force derived from the LP/MT method by

$$\mathrm{re}(t_k) = u_s^*(t_k) - u(t_k) \tag{32}$$

Then the gain matrix G in Eq. (31) is selected to minimize

$$\mathrm{RE} = \sum_{k=1}^{N} [\mathrm{re}(t_k)]^2 \tag{33}$$

To insure stability in the linear region, consider only the gain matrix

$$G = R^{-1}B^T S \tag{34}$$

which is derived from the algebraic Riccati Equation[15] in S

$$A^T S + SA - SBR^{-1}B^T S + Q = O \tag{35}$$

where Q and R are weighting matrices that are to be chosen by an iterative process. The feedback gain matrix G of Eq. (34) results in a solution that minimizes the quadratic performance index

$$J = \int_0^\infty (s^T Q_s + u^T R u)\, \mathrm{d}t \tag{36}$$

while Q and R are chosen to minimize the mean-square difference RE in Eq. (33).

Application of the Suboptimal Method

As an example, the problem that has been analyzed by the limiting-performance method is also analyzed by deriving a suboptimal control law. The direction-set method[16] in multidimensional parameters is employed to find u_s^* (a scalar in this example) from Eq. (30) by specifying matrix R, and then varying matrix Q to calculate G from Eq. (34) and u_s^* from Eqs. (29–31) until the residual RE in Eq. (33) is minimized. To get a unique solution, only diagonal matrices Q are considered.

Choose

$$R = 0.0001 \tag{37}$$

For the optimal solution presented in Fig. 8, the following matrix Q is found to minimize Eq. (33):

$$Q = \begin{bmatrix} 6.0 & 0.0 & 0.0 & 0.0 \\ 0.0 & 0.08 & 0.0 & 0.0 \\ 0.0 & 0.0 & 1.0 & 0.0 \\ 0.0 & 0.0 & 0.0 & 0.04 \end{bmatrix} \tag{38}$$

The resultant feedback gain matrix is

$$G = [242.646 \quad -26.615 \quad -100.022 \quad -24.062] \tag{39}$$

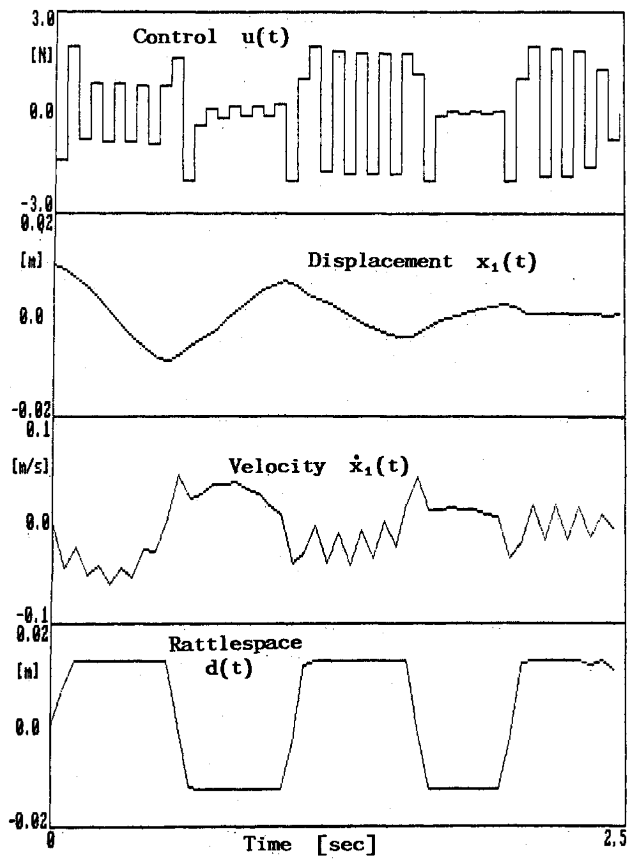

Fig. 8 The LP/MT characteristics.

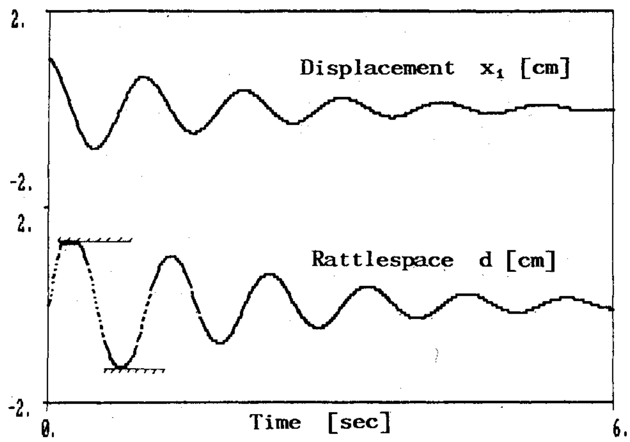

Fig. 9 Time response of a suboptimal feedback control system.

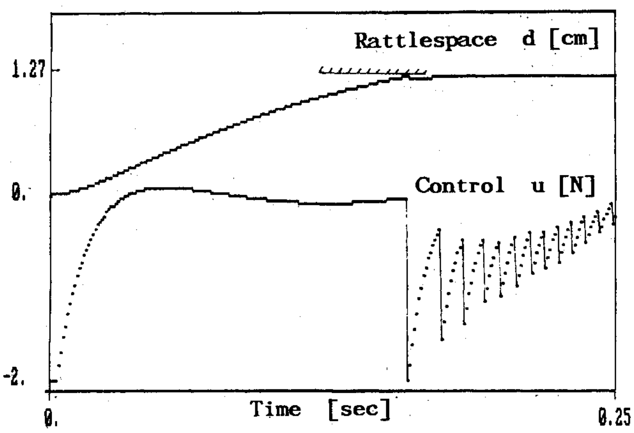

Fig. 10 Magnified detail from Fig. 9 showing elastic impacts.

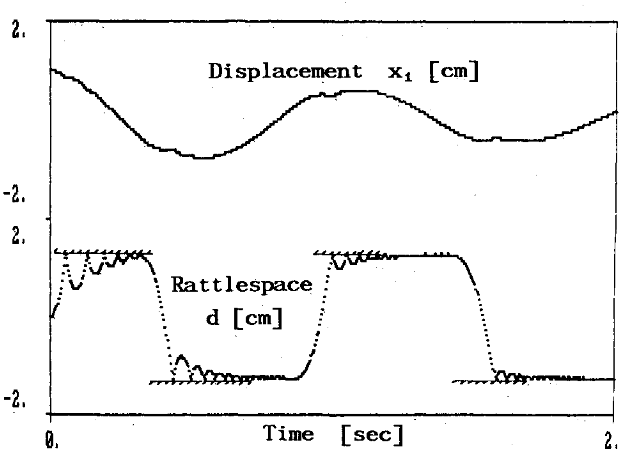

Fig. 11 Time response of a nonoptimal feedback control system.

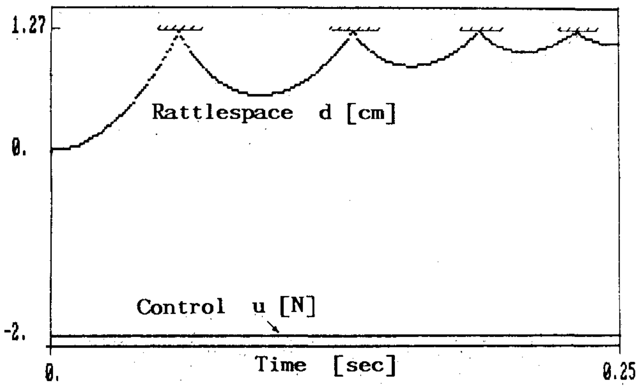

Fig. 12 Magnified detail from Fig. 11 showing elastic impacts.

and the closed-loop eigenvalues are

$$-79.58, \quad -5.03, \quad -0.52 \pm 5.94i \tag{40}$$

The time response for an initial condition $x_1(t_0) = 0.01$ m has been integrated numerically and is given in Fig. 9. The effects of impacts between the proof mass and a stop are shown magnified in Fig. 10. There are repeated rebounds on impact followed by acceleration of the proof mass back toward the stop as the effects of the control forces are felt. The suboptimal feedback gains of Eq. (39) provide control forces that minimize the influence of impacting, and the results obtained indicate that the limiting performance solution is reasonably accurate even though impact dynamics have been replaced by holding the proof mass off the stops. The control system is able to damp out the initial displacement within less than 6 s. For the first two seconds, the results are close to the limiting-performance solution shown in Fig. 8. More time is needed to damp the vibration in the linear region.

For comparison, we look at the nonoptimal case. Choose the feedback gain matrix

$$G = [928.62 \quad -57.61 \quad -31.62 \quad -12.90] \tag{41}$$

which is far from the optimal solution, but results in stable eigenvalues

$$-13.16 \pm 14.46i, \qquad -1.99 \pm 2.79i \tag{42}$$

The results for this nonoptimal case are shown in Figs. 11 and 12 as a comparison to the results shown in Figs. 9 and 10. In the nonoptimal case, a longer time is spent in wall impacts than before, resulting in poorer damping.

Summary and Conclusions

A linear control law for the proof-mass damper was studied that would provide adequate damping over the full frequency range, so that it would act as a self-contained damper. Although adequate damping at high frequencies was possible, it was shown that the linear control law would be ineffective at low frequencies, i.e., in the vicinity of 1 Hz, due to the stroke limits of the proof-mass dampers. The limiting-performance method was used in a preliminary study of a method to improve low-frequency damping. To provide rapid suppression of the structural vibration, the limiting-performance method was formulated for minimum time and was applied to a single-degree-of-freedom model of a cantilever beam controlled by a proof-mass damper. Optimal response trajectories were obtained, which could be considered as the best possible response of the system. For the practical application of the limiting-performance method, the construction of a feedback control based on the optimal trajectories was studied and, in this case, elastic impacts with the steps were incorporated. A parameter identification technique incorporating the Riccati equation was employed to find suboptimal feedback control gains. Numerical simulation with these gains showed that even though the proof mass impacted the stops, no instability or serious adverse effect on the damping was observed. Although examples were given for 1 Hz, actuators with different physical characteristics than the prototype analyzed would be subject to scaling laws; thus, comparable results would have been obtained at different frequencies. Further, the system as presented is not adaptive; consequently, it would only be effective when tuned to a particular beam frequency. Future work will concentrate on methods of removing this restriction.

Acknowledgment

This work was supported by the Air Force Office of Scientific Research, Washington, DC.

References

[1]Balas, M. J., "Trends in Large Space Structure Control Theory: Fondest Hopes, Wildest Dreams," *IEEE Transactions on Automatic Control,* Vol. AC-27, No. 3, June 1982, pp. 522–535.

[2]Aubrun, J. N., Ratner, M. J., and Lyons, M. G., "Structural Control for a Circular Plate," *Journal of Guidance, Control, and Dynamics,* Vol. 7, No. 5, Sept.-Oct. 1984, pp. 535–545.

[3]Davis, L. D., Hyland, D. C., Otten, T., and Ham, F. M., "Mast Flight System Dynamic Performance," *Proceedings of the First NASA/DOD CSI Technology Conference,* NASA CP 2447, Nov. 1986, pp. 281–298.

[4]Shipley, J. W., and Hyland, D. C., "The Mast Flight System Dynamic Characteristics and Actuator/Sensor Selection and Location," *Proceedings of the 9th Annual AAS Guidance Control Conference,* edited by R. D. Culp and J. C. Durrett, American Astronautical Society, San Diego, CA, 1986, pp. 31–49.

[5]Shipley, J. W., Davis, L. D., Burton, W. T., and Ham, F. M., "Development of the Mast Flight System Linear DC Motor Inertial Actuator," *Proceedings of the 10th Annual AAS Guidance Control Conference,* edited by R. D. Culp and T. J. Kelley, American Astronautical Society, San Diego, CA, 1987, pp. 237–255.

[6]Ham, F. M., and Greeley, S. W., "Active Damping Control Design for the Mast Flight System," *Proceedings of the American Control Conference,* American Automatic Control, Piscataway, NJ, distributed by IEEE Service Center, June 1987, pp. 355–367.

[7]Ham, F. M., Henniges, B. L., and Greeley, S. W., "Active Damping Control Design for the COFS Mast Flight System," *Proceedings of the AIAA Guidance, Navigation, and Control Conference,* AIAA, New York, 1987, pp. 354–360.

[8]Zimmerman, D. C., Inman, D. J., and Horner, G. C., "Dynamic Characterization and Microprocessor Control of the NASA/UVA Proof Mass Actuator," AIAA Paper 84-1077, May 1984.

[9]Salehi, S. V., and Ryan, E. P., "On Optimal Nonlinear Feedback Regulation of Linear Plants," *IEEE Transactions on Automatic Control,* Vol. AC-27, No. 6, Dec. 1982, pp. 1260–1264.

[10]Haviland, J. K., Politansky, H., Lim, T. W., and Pilkey, W. D., "The Control of Proof-Mass Dampers," *Proceedings of the Sixth VPI&SU/AIAA Symposium on Dynamics and Control of Large Structures,* Virginia Polytechnic Inst. and State Univ., Blacksburg, VA, 1987, pp. 201–216.

[11]Haviland, J. K., Lim, T. W., Pilkey, W. D., and Politansky, H., "The Control of Linear Dampers for Large Space Structures," *Proceedings of the AIAA Conference on Guidance, Navigation, and Control,* AIAA, New York, 1987, pp. 106–116.

[12]Sevin, E., and Pilkey, W. D., *Optimal Shock and Vibration Isolation,* Shock and Vibration Information Center, Washington, DC, 1971.

[13]Politansky, H., and Pilkey, W. D., "Suboptimal Feedback Vibration Control of a Beam with a Proof-Mass Actuator," *Proceedings of the AIAA Conference on Guidance, Navigation, and Control,* AIAA, New York, 1987, pp. 370–378; also, *Journal of Guidance, Control, and Dynamics* (to be published).

[14]Ortega, J. M., and Poole, W. G., Jr., *An Introduction to Numerical Analysis for Differential Equations,* Pitman, Aulander, NC, 1981, pp. 124–135.

[15]Lewis, F. L., *Optimal Control,* Wiley, New York, 1986.

[16]Press, W. H., Flannery, B. P., Teukolsky, S. A., and Vetterling, W. T., *Numerical Recipes: The Art of Scientific Computing,* Cambridge Univ. Press, New York, 1987.